



Self-Shielding Gyroscopic Radiosurgery—A First Clinical Experience, Case Series, and Dosimetric Comparison

Alexander Muacevic¹, Michael Martin Eder¹, Theresa Hofmann¹, Christoph Fürweger^{1,2}, Felix Ehret^{1,3,4}

BACKGROUND: Self-shielding gyroscopic radiosurgery (GRS) represents a technical innovation in the field of stereotactic radiosurgery. GRS does not require a radiation vault and is optimized for radiosurgical treatments. Reports on its usage are limited. We describe the first clinical experience of GRS at our institution to assess the application of GRS in the treatment of cranial tumors. Moreover, we perform a dosimetric comparison to robotic radiosurgery (RRS) with vestibular schwannoma (VS) GRS patients.

METHODS: Patients who were treated with GRS between July and November 2021 were included. Patient, tumor, and dosimetric characteristics were retrospectively summarized and analyzed.

RESULTS: Forty-one patients with 48 intracranial tumors were included. Tumor entities mostly comprised VS, brain metastases, and meningiomas. The median prescription dose and isodose line were 13.5 Gy and 50.0% for benign neoplasia versus 20 Gy and 60.0% for malignant tumors, respectively. The mean planning target volume was 1.5 cubic centimeters. All patients received a single-fraction treatment without encountering any technical setup difficulties. Treatment plan comparisons with RRS revealed comparable plan characteristics, dose gradients, and organs at risk doses. Significant

differences were detected concerning the new conformity index and number of monitor units per treatment (both $P < 0.01$).

CONCLUSIONS: This case series provides more evidence on the usage of self-shielding GRS in the management of cranial tumors. Dosimetric comparisons for VS cases revealed mostly equivalent dosimetric characteristics to RRS. Further clinical and physical analyses for GRS are underway.

BACKGROUND

Stereotactic radiosurgery (SRS) is a versatile and well-established treatment modality for treating various benign and malignant intracranial tumors.¹⁻³ Today, several linear accelerator (LINAC)-based treatment platforms for the delivery of SRS treatments are available. While most of them require a dedicated radiation vault to comply with respective safety requirements, the recently developed self-shielding gyroscopic radiosurgery (GRS) does not require such a vault.⁴⁻⁶ This technical refinement may improve the availability of SRS, thereby meeting the increasing demand for radiotherapy and radiosurgical treatments.^{7,8} The so-called ZAP-X (ZAP Surgical Systems Inc., San Carlos, California, USA) enables radiation oncologists, neurosurgeons, and

Key words

- Case series
- CyberKnife
- Dosimetry
- Gyroscopic radiosurgery
- Stereotactic radiosurgery
- Treatment planning
- ZAP-X

Abbreviations and Acronyms

- GI:** Gradient index
- GRS:** Self-shielding gyroscopic radiosurgery
- HI:** Homogeneity index
- LINAC:** Linear accelerator
- MUs:** Monitor units
- nCI:** New conformity index
- PTV:** Planning target volume
- RRS:** Robotic radiosurgery

- SRS:** Stereotactic radiosurgery
- TPS:** Treatment planning software
- VS:** Vestibular schwannoma

From the ¹European Radiosurgery Center Munich, Munich; ²Department of Stereotaxy and Functional Neurosurgery, University Hospital Cologne, Cologne; ³Berlin Institute of Health at Charité – Universitätsmedizin Berlin, Berlin; and ⁴Charité – Universitätsmedizin Berlin, Corporate Member of Freie Universität Berlin and Humboldt-Universität zu Berlin, Department of Radiation Oncology, Berlin, Germany

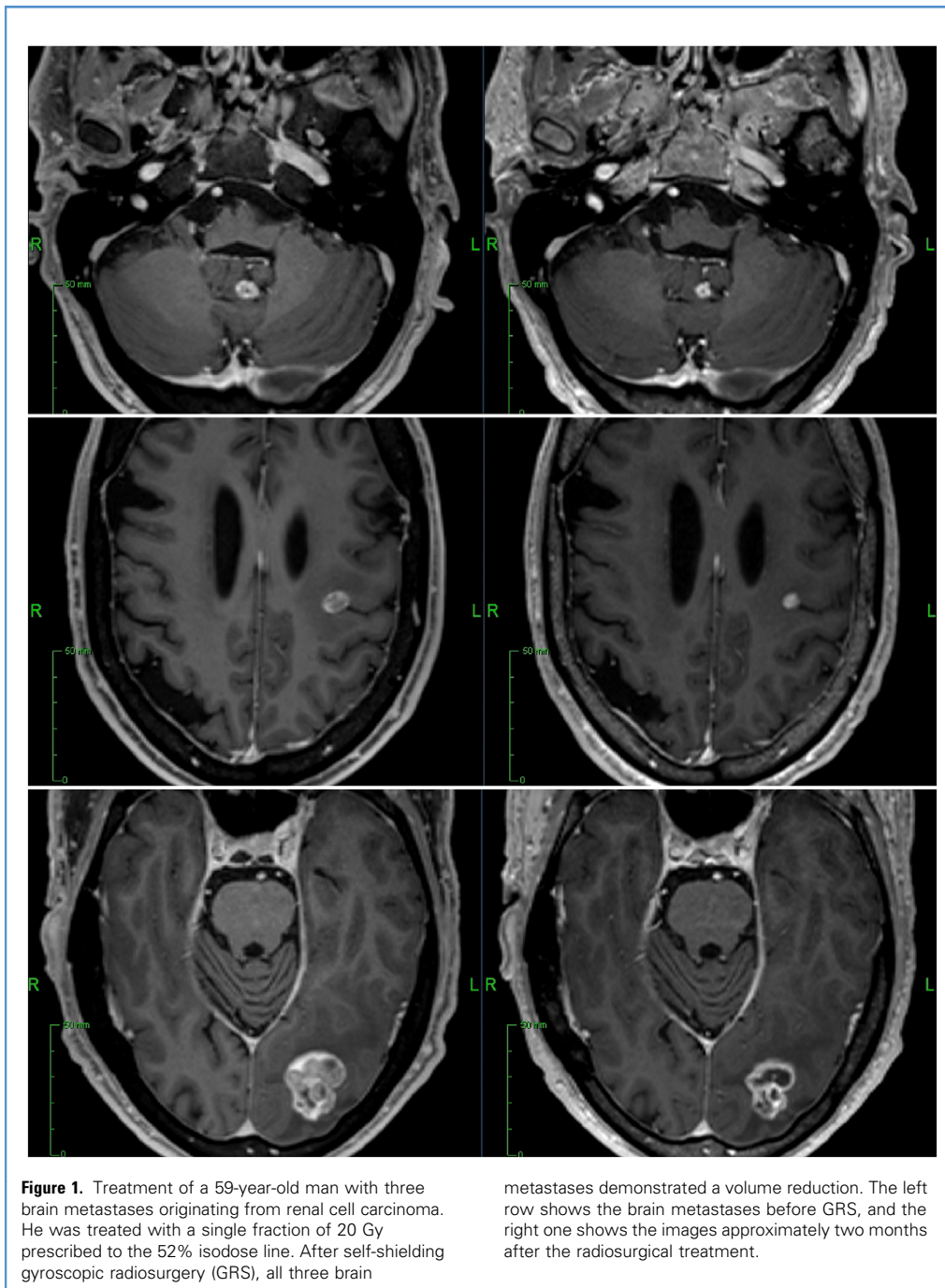
To whom correspondence should be addressed: Felix Ehret, M.D.
[E-mail: felix.ehret@charite.de]

Citation: World Neurosurg. (2022) 164:e420-e426.
<https://doi.org/10.1016/j.wneu.2022.04.120>

Journal homepage: www.journals.elsevier.com/world-neurosurgery

Available online: www.sciencedirect.com

1878-8750/\$ - see front matter © 2022 Elsevier Inc. All rights reserved.



radiosurgeons to perform intracranial GRS. So far, first results and reports on the use of GRS during the clinical routine are scarce. Evidence is currently limited to a technical case report with two patients and a first case series.^{9,10} The objective of this study is to report the first clinical case series with dosimetric analyses of the

GRS. We compare the GRS dosimetric characteristics of the most treated tumor entity thus far, the vestibular schwannoma (VS), with the ones obtained with robotic radiosurgery (RRS) using the well-established CyberKnife (Accuray Inc., Sunnyvale, California, USA) radiosurgery system.



Figure 2. Treatment results of a 68-year-old man with a metastasized malignant melanoma and brain metastasis in the left cerebral peduncle. Self-shielding gyroscopic radiosurgery (GRS) was delivered with a

prescription dose of 20 Gy, prescribed to the 57% isodose line. Three months after GRS, the metastasis significantly decreased in size.

METHODS

Patients who were treated with GRS for an intracranial tumor between July and November 2021 were eligible for this single-center, retrospective analysis. The respective diagnosis of an intracranial pathology was made histopathologically or radiographically. The development, setup, and technical details of self-shielded GRS with the ZAP-X (ZAP Surgical Systems Inc., San Carlos, California, USA) were previously described elsewhere.^{4,6,11} Briefly, the ZAP-X consists of a compact 3 MV LINAC mounted on coupled gimbals allowing for noncoplanar beam delivery, a collimator wheel with 8 circular apertures, and a kV image-guidance system. Before GRS, treatment planning imaging with computed tomography and magnetic resonance imaging was acquired. Patient, tumor, treatment, and dosimetric characteristics were recorded and stored in a dedicated database for SRS treatments. Descriptive statistics utilize ranges, quartiles, median, and mean for continuous variables. For categorical variables, frequencies with percentages are reported. Treatment plan comparisons between GRS and RRS were executed for the available VS cases, focusing on dosimetric quality measures such as the new conformity index (nCI), homogeneity index (HI), dose gradient, and dose to adjacent organs at risk such as the brainstem and cochlea. The nCI is computed as

$$\text{nCI} = \frac{\text{TV} * \text{PIV}}{\text{TV}_{\text{PIV}}^2}$$

where PIV is the total tissue volume that receives the prescription isodose or more, TV_{PIV} is the tumor volume that receives the prescription isodose or more, and TV is the total tumor volume.¹² The HI is defined as

$$\text{HI} = \frac{D_{\text{max}}^{\text{tumor}}}{D_{\text{Rx}}}$$

where $D_{\text{max}}^{\text{tumor}}$ is the maximum tumor dose and D_{Rx} the prescription

dose.¹³ To evaluate the dose gradient, we calculated the gradient index (GI) which is defined as

$$\text{GI} = \frac{\text{hPIV}}{\text{PIV}}$$

where PIV is defined as above and hPIV is the total tissue volume that receives half of the prescription dose or more.¹⁴

Target delineation was done using the Precision planning software (Accuray Inc., Sunnyvale, California, USA). GRS plans were calculated with the integrated ZAP-X treatment planning software (TPS) (version 1005). Optimization of GRS plans was achieved by manual placement of isocenters in the target, followed by several iterations of inverse beam weight optimization and manual adding, removing, or repositioning isocenters. RRS plans for comparison were calculated using the Precision planning software (version 3.1.0.0) for the CyberKnife M6 FIM, which employs a 6 MV LINAC. Due to the small target size, fixed cone collimators or the Iris variable aperture collimator was selected, in all cases using the VOLO optimization technique. To maintain comparability, RRS plans were prescribed to achieve the same target coverage as the GRS plan delivered to the patient. For the comparison of monitor units (MUs), their machine-specific definition—usually referred to as system calibration—is based on similar concepts between ZAP-X and CyberKnife treatment devices. The reference point was set to the maximum of the respective depth dose curve (i.e., 7 mm for ZAP-X and 15 mm for CyberKnife) for both systems at source-axis distance 45 cm for ZAP-X and 80 cm for CyberKnife. System calibration was performed using the machine-specific reference field (i.e., 25-mm circular collimator for ZAP-X and 60-mm fixed cone collimator for CyberKnife) such that 100 MUs yield an energy dose of 1 Gy at the reference point. Comparison of plan metrics was performed with the platform-independent software SciMoCa (Scientific RT, Munich, Germany) to preclude any bias or different interpretation

Table 1. Patient and Treatment Characteristics

Total number of patients	41		
Total number of tumors	48		
Tumor type, benign (%)/malignant (%)	35 (72.9%)/13 (27.1%)		
Sex, male (%)/female (%)	15 (36.6%)/26 (63.4%)		
	Median	Mean	Range
Age (years)	57.9	57.6	13.4–84.5
Planning target volume (cc)	0.9	1.5	0.1–9.4
Benign lesions/tumors			
Prescription dose (Gy)	13.5	14.4	13.0–20.0
Prescription isodose line (%)	50.0	51.6	40.0–65.0
Coverage (%)	97.8	97.3	86.8–99.4
Malignant lesions/tumors			
Prescription dose (Gy)	20	19.9	19–21
Prescription isodose line (%)	60.0	60.1	44.4–75.8
Coverage (%)	99.4	99.3	98.0–100
New conformity index	1.23	1.26	1.11–1.67
Gradient index	2.94	3.04	2.51–4.33
Homogeneity index	1.92	1.89	1.32–2.50
MUs	10,929	12,125	4453–26,166
Number of beams	109	115	41–241
Number of isocenters	8	8	2–15
Tumor/Lesion Entity	Number of Patients		
Vestibular schwannoma	20		
Meningioma	9		
Brain metastases	7		
Pituitary adenoma	2		
Arteriovenous malformation	1		
Neurocytoma	1		
Hemangioma	1		
cc, cubic centimeters; Gy, gray; MUs, monitor units.			

of Digital Imaging and Communications in Medicine objects.¹⁵ A preclinical test release of this software was also employed to verify the dose distributions produced by the GRS and RRS planning software by independent, Monte-Carlo–based dose calculations using gamma (2%/1 mm) analysis. Differences in continuous variables were assessed using the Wilcoxon rank-sum test. The statistical significance was defined as a *P* value of ≤ 0.05 . Given the explorative nature of the work, no adjustments for multiple comparisons were applied. Statistical analyses were performed with STATA MP 16.0 (StataCorp, College Station, TX, USA) and Python SciPy (version 1.32).¹⁶ This study was approved by the local institutional review board.

RESULTS

Patient and Treatment Characteristics

A total of 41 patients with 48 intracranial lesions were included herein. The median age at treatment was 57.9 years. Most patients were female (26 patients). Treated tumor entities included VS, meningioma, brain metastases, neurocytoma, pituitary adenoma, hemangioma, and arteriovenous malformations. A clinical and radiographic follow-up was available for 5 patients. Two representative cases of patients suffering from brain metastases are shown in **Figures 1** and **2**. The median prescription dose and isodose line for benign lesions were 13.5 Gy and 50.0% versus 20 Gy and 60% for malignant lesions, respectively. The planning target volume (PTV) ranged from 0.1–9.4 cubic centimeters, averaging 1.5 cubic centimeters. The median nCI and HI were 1.23 and 1.92, respectively. The dose coverage was between 86.8% and 100%, with a median of 97.8% for benign lesions and 99.4% for malignant tumors. The reported minimum coverage of 86.8% was the only value below 94.0% and occurred during an arteriovenous malformation treatment. All patients received a single-fraction treatment. All patients underwent a short neurological evaluation immediately after the procedure which was documented in the patient charts. No short-term deficits or negative patient experience was observed or reported. Patient characteristics are summarized in **Table 1**.

Dosimetric Comparisons

Twenty patients treated with GRS for a VS were selected for a treatment plan comparison (**Figure 3**). Obtained imaging data were uploaded to the Precision planning software (Accuray Inc., Sunnyvale, California, USA) with subsequent RRS planning. Overall, plan quality was equivalent between GRS and RRS. In particular, there was no significant difference in treatment time, number of beams, mean and maximum PTV dose, mean and maximum cochlea dose, the volume of the brainstem receiving at least a dose of 8 Gy, HI, and GI. Significant differences were detected solely regarding the nCI and MUs per treatment ($P = 0.0001$, $P = 0.0012$, respectively; **Figure 4**). In Monte-Carlo–based secondary dose verification, all GRS and RRS plans yielded gamma pass rates (2%/1 mm, dose cutoff 5%) of $>90\%$. However, while the lowest gamma pass rate in RRS plans was 97.7%, there were six GRS plans with a pass rate of $<95\%$ caused by discrepancies in peripheral low-dose regions. Details of the dosimetric comparison between GRS and RRS are summarized in **Table 2**.

DISCUSSION

Herein, we report the first extensive clinical case series and dosimetric experience of GRS in the management of various intracranial tumors thus far. With the installation of more and more GRS treatment platforms, the number of reports on the clinical effectiveness, treatment setup, and dosimetric features of GRS increases.^{9,10,17,18} Despite the limited sample size and follow-up duration of this report, our first GRS experience is favorable. We selected the VS as the most treated entity thus far to perform a dosimetric comparison between GRS and RRS. Concerning the treatment of VS, SRS is a common and well-established treatment

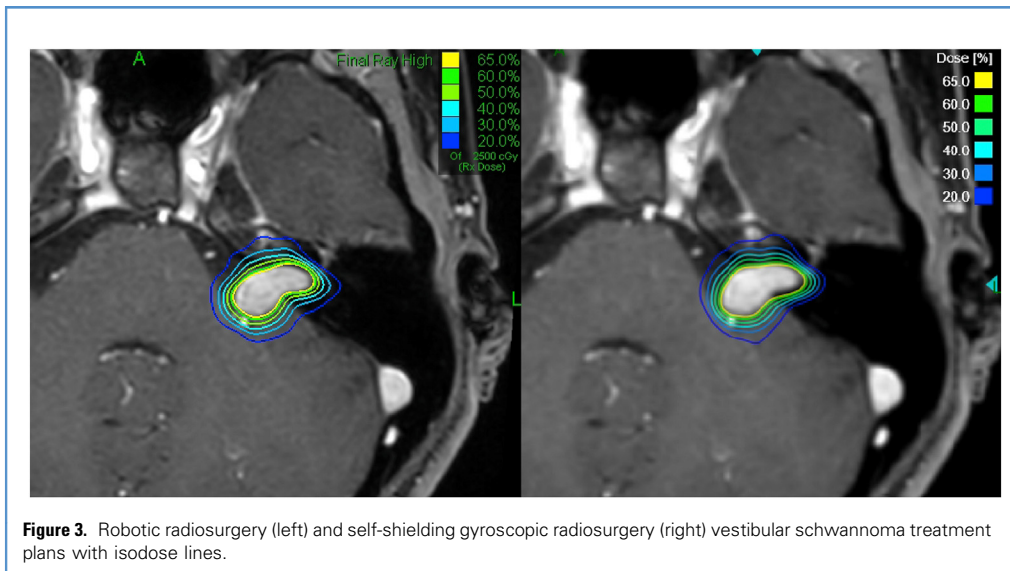


Figure 3. Robotic radiosurgery (left) and self-shielding gyroscopic radiosurgery (right) vestibular schwannoma treatment plans with isodose lines.

modality.¹⁹ Thus, the VS represents a well-suited example for a first investigation. In terms of RRS, one must note that the system is capable of performing extracranial stereotactic body radiotherapy in contrast to GRS, which is only limited to cranial SRS.

Our comparison of GRS and RRS reveals equivalent plan characteristics with regard to doses to adjacent organs at risk, dose to the target, gradient, and treatment time. Statistical differences could only be ascertained for the number of MUs and the nCI. The increase of MUs required in GRS by approximately 15% is expected because the lower maximum beam energy results in higher attenuation when traversing through tissue. Conformity of the dose distribution is affected by the placement of candidate beams as a starting point for inverse optimization of beam weights. Clinical GRS plans were exclusively achieved by manual

isocenter placement and careful iterative refinement of their positions by the user. While the GRS treatment planning system

Table 2. Dosimetric Comparison Between Self-Shielding Gyroscopic Radiosurgery and Robotic Radiosurgery for Vestibular Schwannoma Patients

Variable	Total number of VS patients		P Value
	GRS	RRS	
PTV (cc)	0.74 (0.34–1.37)	0.74 (0.34–1.37)	0.4779
Total MUs	10,096 (8256–11,835)	8783 (7597–9755)	0.0012
Number of beams	96 (115–855)	89 (75–102)	0.0673
Treatment time (minutes)	30 (26–34)	28 (27–30)	0.1018
D _{mean} PTV (Gy)	17.8 (16.9–18.6)	17.8 (17.4–18.2)	0.5755
D _{max} PTV (Gy)	26.0 (23.4–27.8)	25.7 (24.6–26.8)	0.6291
D _{mean} cochlea (Gy)	3.45 (1.79–3.75)	2.63 (2.45–3.67)	0.7652
D _{max} cochlea (Gy)	7.07 (3.67–10.21)	6.12 (3.77–11.39)	0.1169
V _{8Gy} brainstem (cc)	0.02 (0.00–0.09)	0.01 (0.00–0.09)	0.0558
Gradient index	2.97 (2.83–3.25)	3.04 (2.82–3.35)	0.2627
New conformity index	1.36 (1.29–1.46)	1.15 (1.12–1.18)	0.0001
Homogeneity index	2.00 (1.80–2.09)	1.96 (1.89–2.05)	0.6724
V _{10Gy} healthy tissue (cc)	0.52 (0.31–0.97)	0.62 (0.27–0.94)	0.4778

VS, vestibular schwannoma; GRS, self-shielding gyroscopic radiosurgery; RRS, robotic radiosurgery; PTV, planning target volume; cc, cubic centimeters; MUs, monitor units; D, dose; max, maximum; Gy, gray; V, volume.

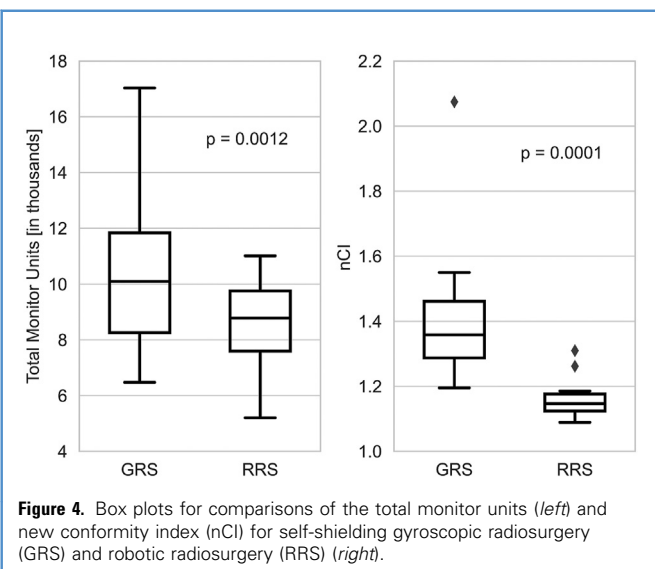


Figure 4. Box plots for comparisons of the total monitor units (left) and new conformity index (nCI) for self-shielding gyroscopic radiosurgery (GRS) and robotic radiosurgery (RRS) (right).

offers basic heuristics for automatic beam placement, the resulting plans were inferior and routinely discarded in favor of plans with user-specified isocenters for clinical treatments. Still, GRS plans exhibited lower conformity than RRS plans. Since both devices have access to circular beams of similar size and shape distributed over a large solid angle, this was not expected a priori. A potential explanation would be that the refined, more mature beam placement heuristics in the RRS treatment planning system were able to generate a superior beam set compared to manual isocenter positioning by the human planner for GRS. GRS plans also showed lower dosimetric accuracy in the periphery, which originated from the coarse calculation resolution of $5 \times 5 \times 5$ mm voxel size employed by the TPS in regions at least 3.2 cm away from the center of any contoured structure. While this was of no clinical concern for the cases treated so far, the global high-resolution calculation of the RRS TPS is preferable.

Besides these first dosimetric evaluations, our clinical experience with GRS was favorable as well. With the introduction of a self-shielding treatment device, several further advantages arise: The possibility that relatives of the patient could join the radiosurgical procedure in the treatment room under natural light was well perceived. Furthermore, and thanks to the treatment setup, no patient stated discomfort during the treatment. These benefits may be particularly valuable for patients who fear radiosurgical procedures or wish to have family and friends close with them during treatment delivery. Besides, the possibility of delivering high-precision radiosurgical treatments without the necessity of dedicated radiation vaults may contribute to the availability of SRS in places where vaults cannot be constructed. So far, SRS and radiotherapy, in general, are mostly limited to high-income countries and respective sites despite the medical demand of such treatments elsewhere.^{7,8} It will be interesting to see how

technological innovations like GRS may shape the future of radiosurgery. Finally, we look forward to upcoming comparisons of different SRS platforms for further insights.

CONCLUSION

This case series provides more evidence on the usage of self-shielding GRS in the management of intracranial benign and malignant tumors. Dosimetric comparisons for 20 VS cases mostly revealed equivalent dosimetric characteristics to RRS. Further clinical and physical in-depth analyses for GRS are underway.

CRediT AUTHORSHIP CONTRIBUTION STATEMENT

Alexander Muacevic: Conceptualization, Funding acquisition, Investigation, Methodology, Project administration, Resources, Supervision, Writing – original draft, Writing – review & editing. **Michael Martin Eder:** Data curation, Formal analysis, Investigation, Methodology, Writing – review & editing. **Theresa Hofmann:** Data curation, Formal analysis, Investigation, Methodology, Writing – review & editing. **Christoph Fürweger:** Conceptualization, Data curation, Formal analysis, Investigation, Methodology, Writing – review & editing. **Felix Ehret:** Conceptualization, Data curation, Formal analysis, Investigation, Methodology, Writing – original draft, Writing – review & editing.

ACKNOWLEDGMENTS

Felix Ehret is a participant in the BIH Charité Junior Clinician Scientist Program funded by the Charité – Universitätsmedizin Berlin and Berlin Institute of Health at Charité (BIH). This work was supported by the German Neurology Foundation (Deutsche Stiftung Neurologie).

REFERENCES

1. Fatima N, Meola A, Ding VY, et al. The Stanford stereotactic radiosurgery experience on 7000 patients over 2 decades (1999-2018): looking far beyond the scalpel. *J Neurosurg.* 2021;135:1721-1745.
2. Yang I, Udawatta M, Prashant GN, et al. Stereotactic radiosurgery for neurosurgical patients: a historical review and current perspectives. *World Neurosurg.* 2019;122:522-531.
3. Chen H, Louie AV, Higginson DS, Palma DA, Colaco R, Sahgal A. Stereotactic radiosurgery and stereotactic body radiotherapy in the management of oligometastatic disease. *Clin Oncol (R Coll Radiol).* 2020;32:713-727.
4. Weidlich GA, Schneider MB, Adler JR. Self-shielding analysis of the Zap-X system. *Cureus.* 2017;9:e1917.
5. Adler JR, Schweikard A, Achkire Y, et al. Treatment planning for self-shielded radiosurgery. *Cureus.* 2017;9:e1663.
6. Weidlich GA, Bodduluri M, Achkire Y, Lee C, Adler JR Jr. Characterization of a novel 3 megavolt linear accelerator for dedicated intracranial stereotactic radiosurgery. *Cureus.* 2019;11:e4275.
7. Yap ML, Zubizarreta E, Bray F, Ferlay J, Barton M. Global access to radiotherapy services: have we made progress during the past decade? *J Glob Oncol.* 2016;2:207-215.
8. Abdel-Wahab M, Gondhowiardjo SS, Rosa AA, et al. Global radiotherapy: current status and future directions-white paper. *JCO Glob Oncol.* 2021;7:827-842.
9. Pan L, Qu B, Bai J, et al. The Zap-X radiosurgical system in the treatment of intracranial tumors: a technical case report. *Neurosurgery.* 2021;88:E351-E355.
10. Hendricks BK, DiDomenico JD, Barani JJ, Barranco FD. ZAP-X gyroscopic radiosurgery system: a preliminary analysis of clinical applications within a retrospective case series. *Stereotact Funct Neurosurg.* 2022;100:99-107.
11. Weidlich GA, Chung W, Kolli S, Thirunarayanan I, Loysel T. Characterization of the ZAP-X® peripheral dose fall-off. *Cureus.* 2021;13:e13972.
12. Nakamura JL, Verhey LJ, Smith V, et al. Dose conformity of gamma knife radiosurgery and risk factors for complications. *Int J Radiat Oncol Biol Phys.* 2001;51:1313-1319.
13. Shaw E, Kline R, Gillin M, et al. Radiation therapy oncology group: radiosurgery quality assurance guidelines. *Int J Radiat Oncol Biol Phys.* 1993;27:1231-1239.
14. Paddick I, Lippitz B. A simple dose gradient measurement tool to complement the conformity index. *J Neurosurg.* 2006;105(Suppl):194-201.
15. Milder MTW, Alber M, Söhn M, Hoogeman MS. Commissioning and clinical implementation of the first commercial independent Monte Carlo 3D dose calculation to replace CyberKnife M6™ patient-specific QA measurements. *J Appl Clin Med Phys.* 2020;21:304-311.
16. Virtanen P, Gommers R, Oliphant TE, et al. SciPy 1.0: fundamental algorithms for scientific computing in Python. *Nat Methods.* 2020;17:261-272.
17. Pinnaduwaage DS, Srivastava SP, Yan X, et al. Small-field beam data acquisition, detector dependency, and film-based validation for a novel

- self-shielded stereotactic radiosurgery system. *Med Phys.* 2021;48:6121-6136.
18. Srivastava SP, Jani SS, Pinnaduwa DS, et al. Treatment planning system and beam data validation for the ZAP-X: a novel self-shielded stereotactic radiosurgery system. *Med Phys.* 2021;48:2494-2510.

19. Windisch PY, Tonn JC, Fürweger C, et al. Clinical results after single-fraction radiosurgery for 1,002 vestibular schwannomas. *Cureus.* 2019;11:e6390.

Conflict of interest statement: Felix Ehret reports honoraria from Accuray outside the submitted work.

Received 10 March 2022; accepted 27 April 2022

Citation: *World Neurosurg.* (2022) 164:e420-e426.
<https://doi.org/10.1016/j.wneu.2022.04.120>

Journal homepage: www.journals.elsevier.com/world-neurosurgery

Available online: www.sciencedirect.com

1878-8750/\$ - see front matter © 2022 Elsevier Inc. All rights reserved.